Journal of Alloys and Compounds 503 (2010) 454–459

Contents lists available at ScienceDirect

Journal of Alloys and Compounds

journal homepage: www.elsevier.com/locate/jallcom

Electrodeposition of CoNi and CoNiP alloys in sulphamate electrolytes

P. Cojocaru[a,*], L. Magagnin[a], E. Gómez[b], E. Vallés[b]

[a] Politecnico di Milano, Dipartimento di Chimica, Materiali e Ingegneria Chimica “Giulio Natta”, Via Mancinelli, 7, 20131 Milano Italy
[b] Electrodep, Departament de Química Fısica and Institut de Nanociència i Nanotecnologia (IN^{2}UB) de la Universitat de Barcelona, Martí i Franquès 1, 08028 Barcelona Spain

ARTICLE INFO

Article history:
Received 8 June 2009
Accepted 9 May 2010
Available online 19 May 2010

Keywords:
Electrodeposition
Cobalt–nickel alloys
X-ray diffraction
Microhardness
Magnetic properties

ABSTRACT

Magnetic, mechanical and structural characterisation of CoNi and CoNiP electrodeposits has been performed. Bright fine-grained fcc soft-magnetic layers of CoNi have been obtained at the different current densities and bath temperatures used. Alloy formation improves the mechanical properties of coating respect to the single electrodeposited metals. The incorporation of phosphorous in CoNi deposits favoured the deposition process, which occurred at less negative potentials. Moderate phosphorous percentages were obtained but significant modifications in the structure and the magnetic properties were detected. Fcc or hcp CoNiP layers can be obtained as a function of deposition conditions, showing the hcp CoNiP the maximum coercivity values. Fcc CoNiP deposits showed the highest hardness values.

1. Introduction

Magnetic materials have received much attention in recent years because their extensive technological applications in microelectronics industry. A particular research study was focused on ferromagnetic materials [1–4].

In particular, the use of cobalt–nickel system has been extended to some magnetic applications, especially in microsystems technology for manufacture of sensors, actuators or inductors [5–7], and their use has been tested as magneto-optic memory material as very desirable data storage material [8,9]. Cobalt and nickel form a solid solution fact that possibilities “to tailor” the alloy composition. The nickel presence in the alloy although diminishes some cobalt magnetic capabilities as magnetisation of saturation but improves the hardness, making the alloy also useful to other different applications that demand both mechanic and environmental resistance.

Electrodeposition is a versatile low-cost method to obtain alloy films, and it is generally compatible with the fabrication of magnetic components in integrated devices. Furthermore, it allows precise control over films properties and permits deposition of variable geometries. The electrodeposition of cobalt–nickel alloy belongs to the anomalous type [10], in which the less noble metal (Co) is preferentially deposited, as the manner that the obtained deposits contain much higher percentage of cobalt than in the solution.

The electrodeposition of cobalt–nickel alloy is accompanied by coevolution of hydrogen that leads local pH rise near the electrode surface during the alloy deposition process. Sulphamate electrolytes seem to be more stable to pH changes than sulphate and chloride electrolytes being sulphamate the preferred bath of industry [11]. Deposits produced by chloride and sulphate baths are exhaustively studied in the investigation ambits [12–15]. However, not much characterisation work exists for deposits obtained from sulphamate bath.

This work was aimed to investigate at first cobalt–nickel deposition in order to characterise the magnetic properties of deposits obtained from sulphamate bath in presence of additives such saccharine, wetting agent and boric acid. We performed the CoNi deposition at different current densities and temperatures. The dependency on crystallinity, surface morphology and microhardness was discussed. Also the incorporation of phosphorous in the alloy will be analyzed. CoNiP ternary alloy deposits will be prepared at similar conditions of those of CoNi, in order to compare the effect of phosphorous presence on the deposition process and to analyze the properties of the obtained deposits. Moreover, the evaluation of the possibility to extend the results obtained from lab-three-electrode system to and industrial ambit will be tested.

2. Experimental procedure

A sulphamate electrolytic bath (*CoNi solution*) was developed for CoNi deposits preparation (55 g/l nickel sulphamate + 20 g/l cobalt sulphamate + 35 g/l H_3BO_3 + 1.5 g/l saccharine + 0.15 g/l SDS) using sodium dodecylsulphate (SDS) as wetting agent and saccharine as antistressing agent. Ternary CoNiP alloys were simultaneously prepared in similar conditions adding sodium hypophosphite as a source of phosphorous. All the solutions were prepared using water treated with a Millipore Milli Q system. The solution pH was adjusted to 4 using NaOH solution. Electrodeposits were prepared galvanostatically at different current densities and temperatures. Plating solution in a 300 ml cell was mechanically stirred (200 rpm) using a mechanical stirrer. A programmable EG&G galvanostat/potentiostat was

---

* Corresponding author. Tel.: +39 0223993150; fax: +39 0223993180.
E-mail address: paula.cojocaru@polimi.it (P. Cojocaru).

0925-8388/$ – see front matter © 2010 Elsevier B.V. All rights reserved.
doi:10.1016/j.jallcom.2010.05.032

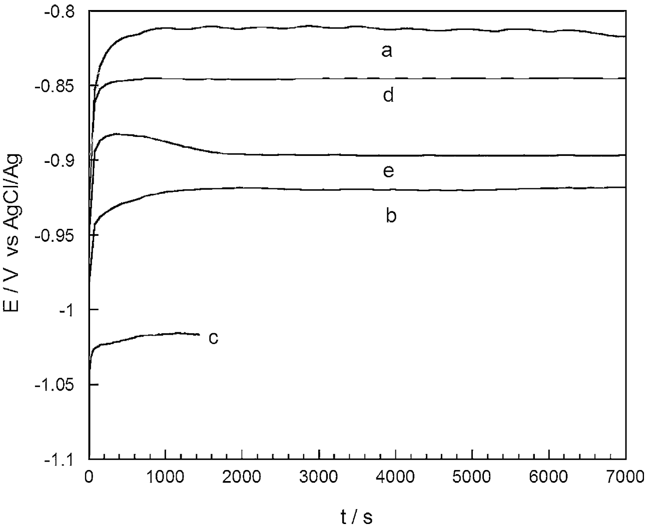

Fig. 1. *E*–*t* transients of CoNi electrodeposition at different current densities (*j* in mA cm^{-2}) and temperatures (°C) (a) $j = -10$, $T = 50$, (b) $j = -30$, $T = 50$, (c) $j = -50$, $T = 50$, (d) $j = -10$, $T = 40$, (e) $j = -10$, $T = 30$.

used with Ag/AgCl as reference electrode and a commercial nickel–sulphur anode as counterelectrode. Deposits 10 μm thick were obtained over inox steel substrate polished with grit paper prior the electrodeposition. Samples were detached of the substrate for posterior characterisation. For all conditions samples were prepared in triplicate in order to assure reproductibility.

Elemental analysis of the deposits was performed with a Fischerscope X-ray XAN and confirmed with a scanning electron microscope Zeiss EVO 50 equipped with microanalysis. Deposit morphology was observed using Hitachi S 2300 scanning electron microscope.

The phase analysis of the deposits was studied by X-ray powder diffractometry (XRD), using a Siemens D-500 diffractometer in conventional Bragg–Brentano configuration. The Cu Kα radiation (λ = 1.5418 Å) was selected using a diffracted beam curved graphite monochromator. The X-ray powder diffraction diagrams were measured in the 5–100° 2θ range with a step range of 0.05° and a measuring time of 15 s per step.

Coatings were characterised in terms of micromechanical properties. Vickers microhardness (HV) data were obtained from penetration depth-load curves by means of a Fischerscope® H100 microhardness measurement system. Measurements conditions were as follows: 250 mN peak load, 10 s loading/unloading time and 5 s holding time at peak load. The reported values are the average of 5 measurements taken on three different samples prepared in the same conditions from the same bath.

Magnetic properties were characterised by means of a SQUID magnetometer at room temperature. Magnetisation vs magnetic field curves of the different samples placed parallel to the magnetic field was recorded.

3. Results and discussion

3.1. Characterisation of CoNi coatings

Films of CoNi were prepared from *CoNi solution* at different temperatures and current densities. Galvanostatic curves reveal the logical dependences of the stabilisation potential as a function of both current density and temperature (Fig. 1). Stabilisation potentials were more negative by applying more negative current densities. At fixed current density (−10 mA cm^{-2}) an increase in the temperature advanced the deposition potential.

Anomalous CoNi deposition was observed for all conditions tested (Table 1) as is usual in the CoNi system from different electrolytic baths used [16,17]. At fixed current density a low decrease of the cobalt percentage was observed when temperature was increased. On the other hand, an increase of the current density favoured the decrease of the cobalt percentage. This behaviour corresponds to a nickel deposition process controlled by activation whereas cobalt deposition process can be controlled by mass transfer as in other media [18].

Table 1
Composition of CoNi electrodeposits as a function of the bath temperature and current density applied.

mA cm^{-2}	°C	at.% Ni	at.% Co
−10	50	47.0	53.0
−30	50	54.2	45.8
−50	50	55.3	44.7
−10	40	44.2	55.8
−10	30	40.2	59.8

Few variations in the morphological, structural and mechanical properties of the CoNi deposits were observed for the different deposition conditions tested. Compact, no fragile and very fine-grained CoNi deposits were always obtained, which morphology was hardly detected from SEM observation (Fig. 2).

XRD results agree with those obtained from SEM micrographs, wide peaks were detected being the calculated grain sizes using Debye–Scherrer equation around 13 nm. All CoNi deposits prepared showed diffraction peaks corresponding to an fcc structure (Fig. 3). No differences were observed in the range of current densities and temperatures used. The position of the peaks of the fcc phase was shifted to lower θ values than those corresponding to pure nickel as a consequence of the incorporation of cobalt in the fcc crystalline lattice. The intermediate position of the peaks between those of cobalt fcc and nickel fcc reveal the formation of solid solution of both metals.

Determination of both HV hardness and Young's modulus was made acquiring measurements on the surface and on the cross section of the films detached. The results show that no significant variation was observed for the alloy deposits as a function of the applied current density. The obtained microhardness values ranged between 533–547 HV with standard deviation SD ≈ 20. In order to compare the mechanical properties of alloy and pure metals, the electrodeposition of both nickel and cobalt was performed from the sulphamate bath containing the corresponding metal in the same operating parameters. Microhardness of obtained CoNi alloy improved: microhardness values were higher than those corresponding to electrodeposited nickel (337 HV with SD ≈ 24) and electrodeposited cobalt (450 HV with SD ≈ 15).

When mechanical properties of the coatings prepared at different temperatures were analyzed, a gradual variation of the values was observed as a function of the deposition temperature. Fig. 4 shows that when the deposition temperature decreases, both the micro hardness and Young's modulus decrease. The maximum

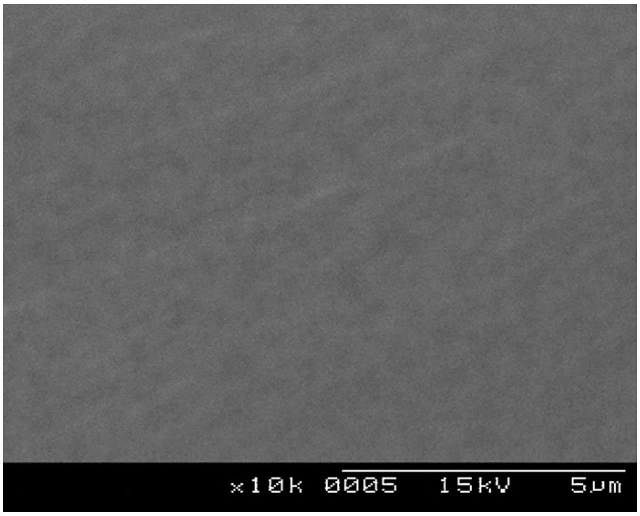

Fig. 2. SEM picture of a CoNi deposit obtained at $j = -10$ mA cm^{-2}, $T = 50$ °C.

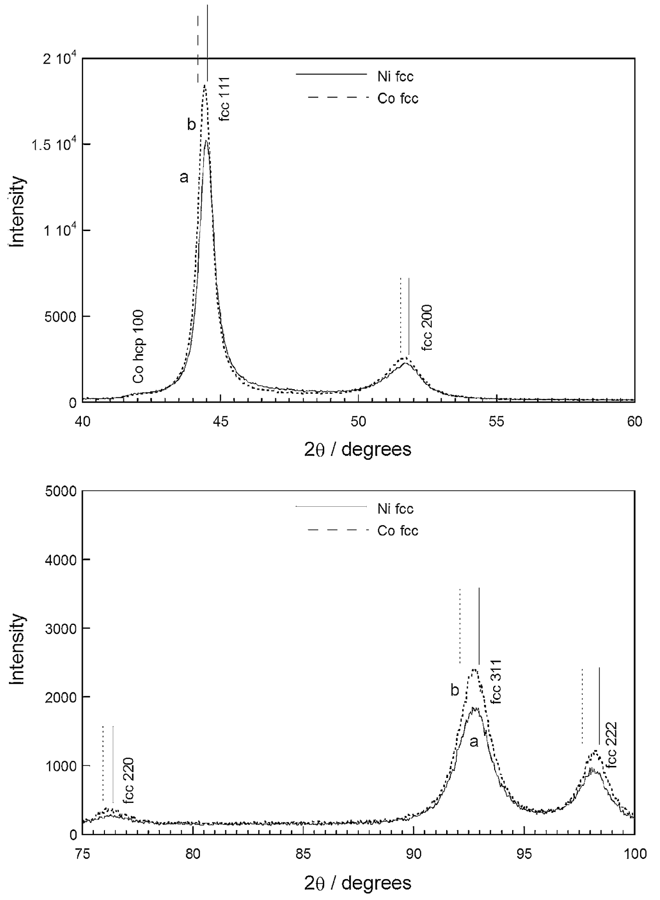

Fig. 3. Two details of the X-ray diffractograms of CoNi deposits obtained at 50 °C and: curve (a) $j = -10\,\mathrm{mA\,cm^{-2}}$, curve (b) $j = -50\,\mathrm{mA\,cm^{-2}}$.

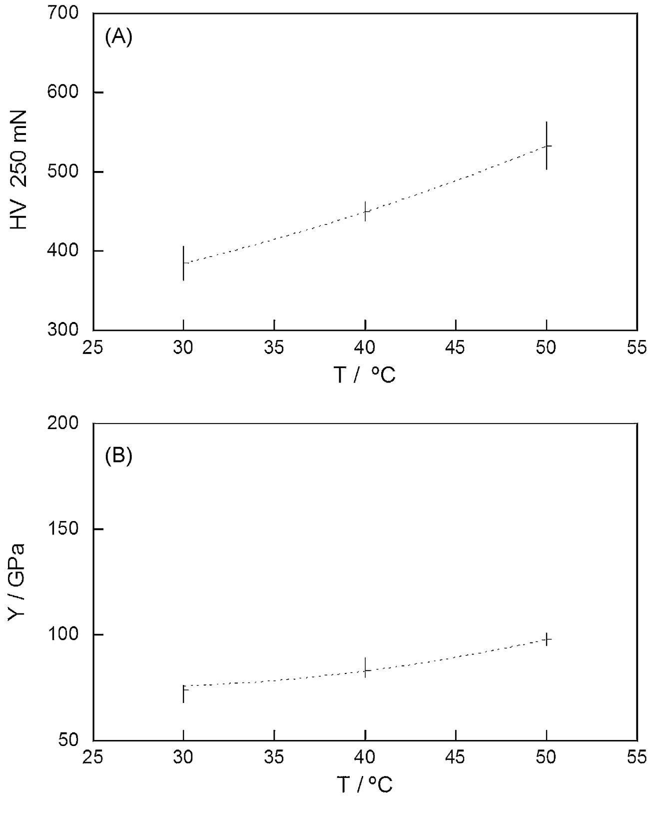

Fig. 4. Dependence of the microhardness (A) and Young's modulus (B) with the temperature for CoNi deposits obtained at $j = -10\,\mathrm{mA\,cm^{-2}}$.

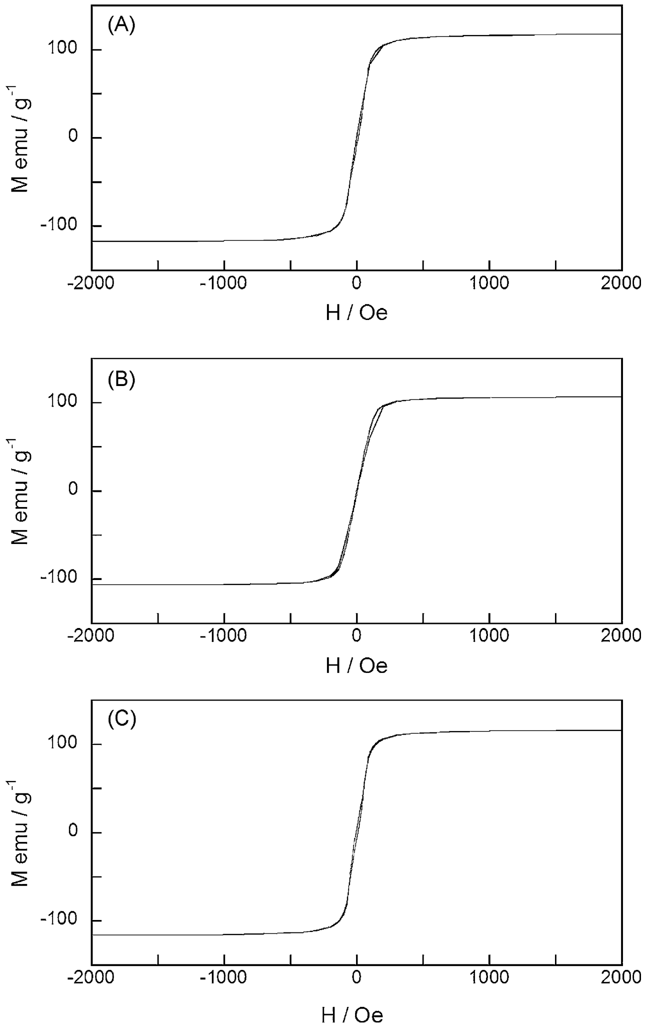

Fig. 5. Magnetisation vs magnetic field applied for CoNi samples prepared at: (A) $j = -10\,\mathrm{mA\,cm^{-2}}$, $T = 50\,°\mathrm{C}$, (B) $j = -50\,\mathrm{mA\,cm^{-2}}$, $T = 50\,°\mathrm{C}$, (C) $j = -10\,\mathrm{mA\,cm^{-2}}$, $T = 40\,°\mathrm{C}$.

hardness (up to 533 HV) and minimum elasticity (98 GPa) was observed for CoNi prepared at the higher temperature used.

In order to study the magnetic properties of alloy prepared, the magnetisation vs applied magnetic field curves were recorded. For all current densities and temperatures used, soft-magnetic properties of the films were detected (Fig. 5). All deposits showed very low coercivity values lower than 10 Oe. The magnetisation of saturation value decreased (from 117 emu $\mathrm{g^{-1}}$ for deposits of 55 at.% Co to 107 emu $\mathrm{g^{-1}}$ for deposits with 45 at.% Co) as the cobalt content decreased due to the lower saturation magnetisation of pure electrodeposited nickel (52 emu $\mathrm{g^{-1}}$) with respect to pure electrodeposited cobalt (150 emu $\mathrm{g^{-1}}$).

3.2. Characterisation of CoNiP coatings

In order to study the effect of phosphor incorporation on the deposit's properties (morphology, structure, mechanical and magnetic) this work was focused in electrodeposition of CoNiP alloys. Ternary CoNiP layers were prepared also galvanostatically from the *CoNi solution* by adding 2.5 g/l sodium hypophosphite as phosphor source. Applied current density and temperature values were those previously used for CoNi preparation.

Galvanostatic curves reveal (Fig. 6) the same gradual dependence of the stabilisation potential as a function of both current density and temperature than the recorded during CoNi prepara-

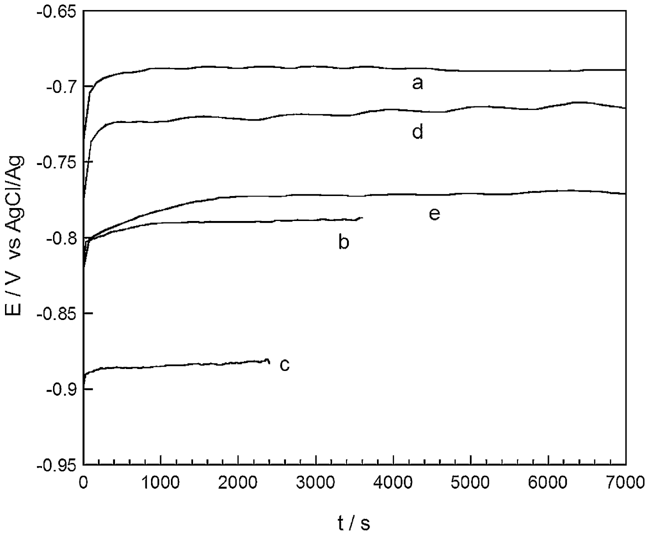

Fig. 6. *E*–*t* transients of CoNiP electrodeposition for different current densities (*j* in mA cm^{-2}) and temperatures (°C). *CoNi solution* + 2.5 g/l sodium hypophosphyte. (a) $j = -10$, $T = 50$, (b) $j = -30$, $T = 50$, (c) $j = -50$, $T = 50$, (d) $j = -10$, $T = 40$, (e) $j = -10$, $T = 30$.

tion. Stabilisation potentials were more negative by applying more negative current densities. At fixed current density (−10 mA cm^{-2}) an increase of temperature advanced the deposition potential. However, the presence of hypophosphite in the solution led to a shift of the deposition stabilisation to less negative values respect to those recorded for CoNi parallel deposit, revealing that the incorporation of some phosphorous in the deposit favour the deposition process.

The presence of hypophosphite in the bath induced phosphorous incorporation in the deposits. In all cases, ternary CoNiP deposition took place, although low incorporation of phosphorous in the deposits was observed (Table 2). In the most conditions, deposits were richer in cobalt revealing that anomalous codeposition between nickel and cobalt was maintained in the presence of hypophosphite in the solution and the dependence of cobalt percentage with temperature was similar than for the binary CoNi deposits. However, normal deposition occurs at −10 mA cm^{-2} and 50 °C.

The CoNiP deposits obtained were compact and fine grained (Fig. 7), but a slight increase in the grain size was observed respect to the corresponding CoNi ones as a consequence of phosphorous incorporation.

Structural modifications were observed in the deposits obtained in the presence of hypophosphite respect to those obtained from free-hypophosphite bath, although crystalline deposits were obtained. The films containing highest nickel percentages presented diffraction peaks assigned to CoNi fcc structure, although the phase was slightly distorted by the presence of the phosphorous and a clear 111 preferred orientation was observed (Fig. 8A). An increase of the estimated grain size up to 22 nm was observed. CoNiP deposits with higher cobalt percentages showed an hcp structure with grain size of around 18 nm. The reflexion peaks slightly shifted to higher θ values respect to those corresponding to pure cobalt, as a consequence of nickel or nickel + phosphorous incorporation in the crystalline lattice of the cobalt phase (Fig. 8B). A certain texture was observed with a 0 0 2 preferred orientation.

Table 2
Composition of CoNiP electrodeposits as a function of the bath temperature and current density applied.

mA cm^{-2}	°C	at.% Ni	at.% Co	at.% P
−10	50	67.5	28.7	3.8
−30	50	44.6	53.6	1.8
−50	50	45.1	53.3	1.6
−10	40	41.4	55.5	3.1
−10	30	33.4	64.0	2.6

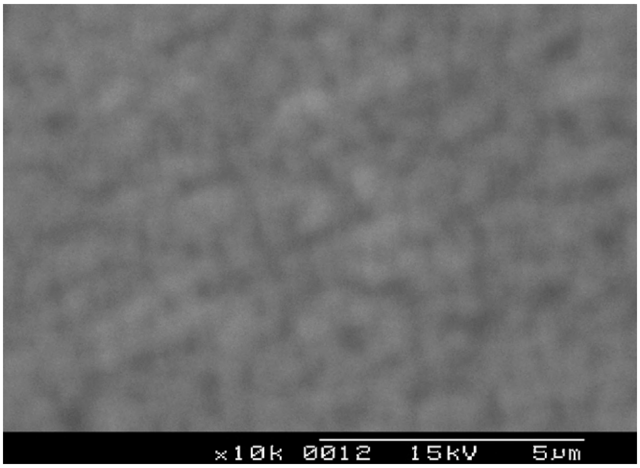

Fig. 7. SEM picture of a CoNiP deposit obtained at $j = -10$ mA cm^{-2}, $T = 50$ °C.

A correlation between the crystalline structure and mechanical behaviour of CoNiP films was found. Phosphorus incorporation led to a slight increase of both HV hardness and Young's modulus, although the tendencies with current density and temperature were similar to those observed for pure CoNi deposits. At fixed deposition temperature, the nickel-rich deposits showing fcc structure presented the highest values of hardness (631 HV with SD ≈ 6).

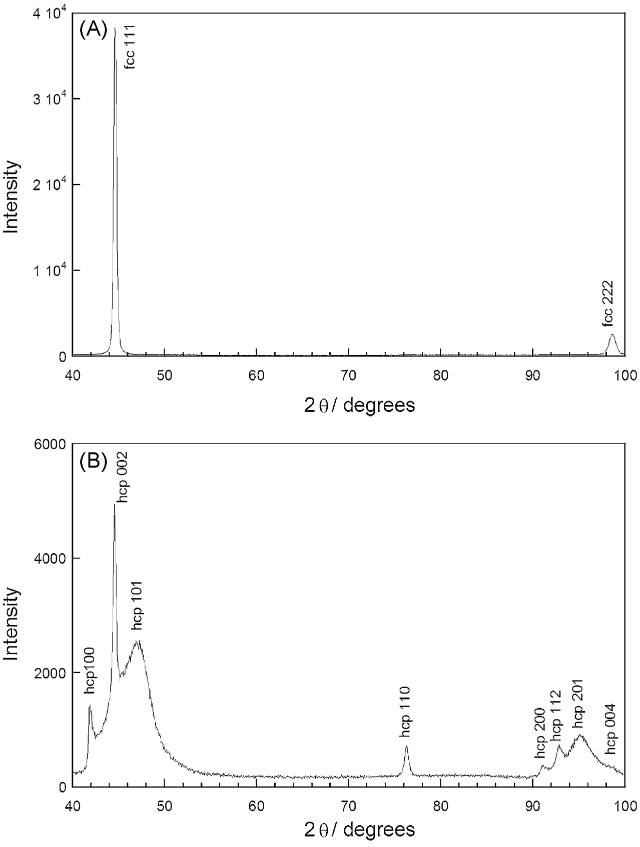

Fig. 8. X-ray diffractograms of CoNiP deposits obtained at 50 °C and: (A) $j = -10$ mA cm^{-2}, (B) $j = -50$ mA cm^{-2}.

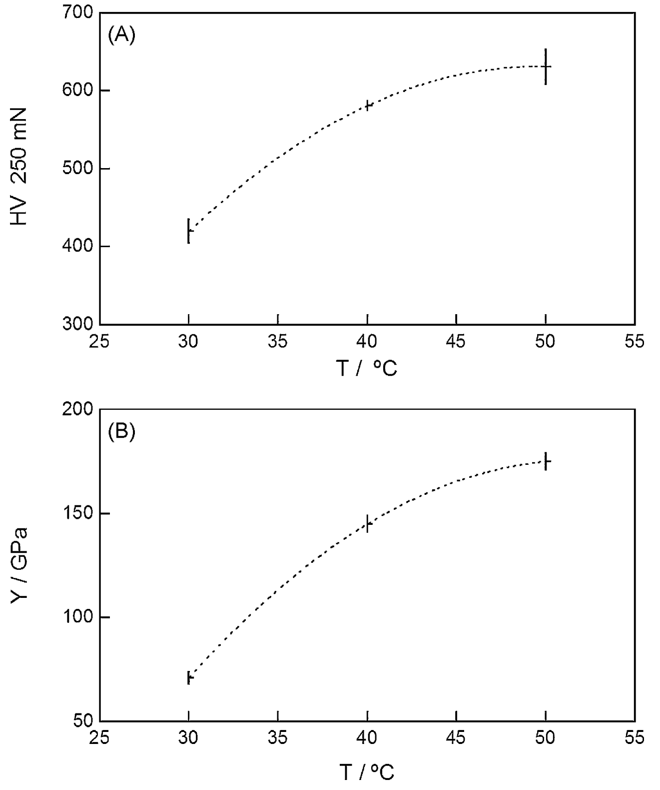

Fig. 9. Dependence of the microhardness (A) and Young's modulus (B) with the temperature for CoNiP deposits obtained at $-10\,\mathrm{mA\,cm^{-2}}$.

By increasing the current density, microhardness decrease and values of around 530 HV were obtained.

When temperature was increased the Young's modulus increases up to 175 GPa (Fig. 9). An important increase of the Young's modulus and microhardness was observed respect to those measured for the corresponding CoNi deposits.

CoNiP nickel-rich deposits were compact and consistent and no damage of the films was observed by detaching the layer from the substrate. However, the other CoNiP deposits prepared were fragile because they easily break down when were detached from the substrate.

The influence of the phosphorous incorporation in the magnetic properties of CoNi deposits was studied by recording magnetisation vs magnetic field curves of coatings prepared at different temperature and current densities. Magnetic curves reflected the change in the crystalline structure observed from XRD characterisation. Deposits with hexagonal phase showed higher values of both coercivity and magnetic susceptibility (Fig. 10).

The comparison of the magnetic properties of the binary CoNi and ternary CoNiP deposits showed that, even maintaining both the cobalt percentage in the deposits and the structural phase (fcc), ternary deposits loose the soft-magnetic behaviour and lowered the susceptibility value observed for CoNi binary deposits prepared at similar deposition conditions (Fig. 11). It seems that the phosphorous presence hinders the magnetic domain orientation.

In order to extend the study of industrial application, parallel experiments were made using a two-electrode system in a tank-cell. The results obtained a lab-scale (three-electrode electrochemical system) have been validated. For the baths studied, the use of the electrochemical system of two-electrodes, led to the same compositional dependences with both the temperature and the current density than those obtained using the system of three electrodes. Moreover, CoNi and CoNiP coatings obtained by electrodeposition was involved in the

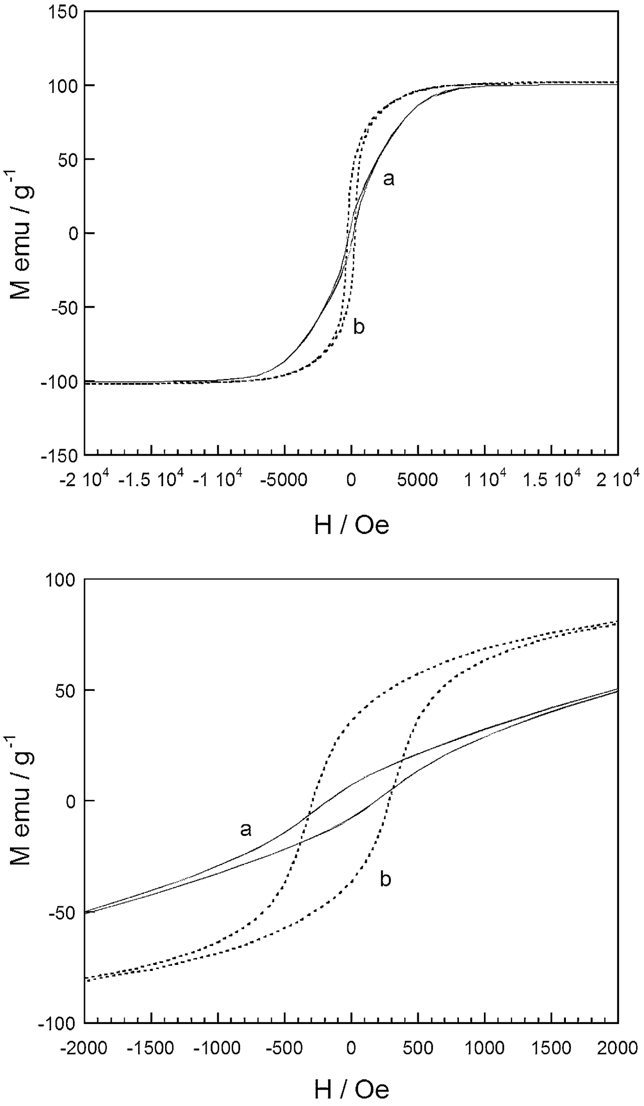

Fig. 10. Magnetisation vs magnetic field applied for different CoNiP samples prepared at fixed temperature (50 °C) at: (a) $j = -10\,\mathrm{mA\,cm^{-2}}$, fcc structure, (b) $j = -50\,\mathrm{mA\,cm^{-2}}$, hcp structure.

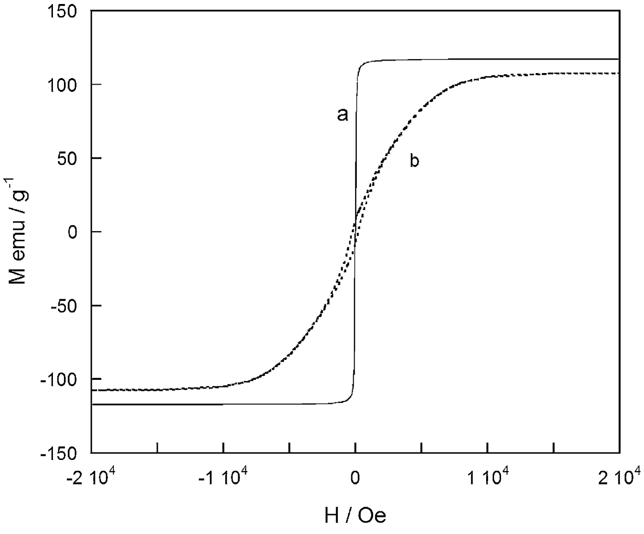

Fig. 11. Magnetisation vs magnetic field applied graph for CoNi (curve a) and CoNiP (curve b) deposits obtained in the same conditions ($j = -10\,\mathrm{mA\,cm^{-2}}$, $T = 40\,^{\circ}\mathrm{C}$).

fabrication (industrial scale) of optic shell for space applications.

4. Conclusions

From the sulphamate bath used, CoNi layers of several microns were compact and fine grained, showing a clear soft-magnetic behaviour with different saturation of magnetisation as a function of their cobalt percentage. No significant variation in their properties was observed when they were prepared from different current densities or temperatures, which led to prepare soft-magnetic non fragile films in a wide range of experimental conditions.

Clear modifications in both magnetic and mechanical properties of CoNi electrodeposits have been observed when hypophosphite was added to the electrodeposition solutions and phosphorous was incorporated in the deposits, although a low phosphorous percentage has been detected in the CoNiP layers. Soft-magnetic behaviour is lost in the presence of phosphorous, especially when the crystalline phase varied from fcc to hcp one and the susceptibility of the films could be modulated. Then, the electrodeposition of CoNi from sulphamate bath but in the presence of sodium hypophosphite allows modulating the magnetic properties of the CoNi layers.

CoNi coating improve the mechanical properties of pure cobalt and pure nickel electrodeposits up to 533 HV. The phosphorous incorporation increases the HV values of the films, but fragility of the coatings was observed. However, fcc CoNiP deposits present higher compactness than hcp ones.

Acknowledgement

EG and EV wish to thank the financial support by contract MAT2006-12913-C02-01 from the *Comisión Interministerial de Ciencia y Tecnología* (*CICYT*) of Spain.

References

[1] B. Lochel, A. Maciossek, J. Electrochem. Soc. 143 (1996) 3343–3348.
[2] T. Wang, A.B. McCandless, R.M. Lienau, K.W. Kelly, D. Hensley, Y. Desta, Z.G. Ling, J. Microelectromech. Syst. 14 (2005) 400–409.
[3] S. Guan, B.J. Nelson, J. Microelectromech. Syst. 15 (2006) 330–337.
[4] R.D. Noce, N. Barelli, R.F.C. Marques, P.T.A. Sumodjo, A.V. Benedetti, Surf. Coat. Technol. 202 (2007) 107–113.
[5] Y. Sverdlov, Y. Rosenberg, Y.I. Rozenberg, R. Zmood, R. Erlich, S. Natan, Y. Shacham-Diamand, Microelectron. Eng. 76 (2004) 258–265.
[6] S. Guan, B.J. Nelson, J. Electrochem. Soc. 152 (2005) C190–C195.
[7] J. Casals-Terré, M. Duch, J.A. Plaza, J. Esteve, R. Pérez-Castillejos, E. Vallés, E. Gómez, Sens. Actuators A 147 (2008) 600–606.
[8] J.N Hilfiker, D.W. Glenn, S. Heckens, J.A. Woollam, K.W. Wierman, J. Appl. Phys. 79 (1996) 6193.
[9] Z.Q. Zou, H. Wang, J. Zhou, D.F. Shen, Y.P. Lee, Eur. Phys. J. B 45 (2005) 97–102.
[10] A. Brenner, Electrodeposition of Alloys. Principles and Practice, Academic Press, New York, 1963.
[11] S. Goldbach, R. de Kermadec, F. Lapicque, J. Appl. Electrochem. 30 (2000) 277–284.
[12] C. Fan, L. Piron, Electrochim. Acta 41 (1996) 1713–1719.
[13] N. Zech, E.J. Podlaha, D. Landolt, J. Electrochem. Soc. 146 (1999) 2886–2891.
[14] L. Burzynska, E. Rudnik, Hidrometallurgy 54 (2000) 133–149.
[15] C.K. Chung, R.X. Zhou, W.T. Chang, Microsyst. Technol. 14 (2008) 1279–1284.
[16] V.D. Jovic, N. Tosic, M. Stojanovic, J. Electroanal. Chem. 420 (1997) 43–51.
[17] E. Gómez, J. Ramírez, E. Vallés, J. Appl. Electrochem. 28 (1998) 71–79.
[18] C. Fan, D.L. Piron, Electrochim. Acta 41 (1996) 1713–1719.